V-shaped Oxydiphthalimides: Side Chain Engineering Regulates Crystallisation-Induced Emission Enhancement

Gopika Gopan,[⊥] P. S. Salini,[⊥] Somadrita Deb and Mahesh Hariharan*

School of Chemistry, Indian Institute of Science Education and Research Thiruvananthapuram, CET Campus, Sreekaryam, Thiruvananthapuram, Kerala, INDIA 695016

Electronic Supplementary Information

Materials and methods:

IR spectra were recorded on a Shimadzu IRPrestige-21 FT-IR spectrometer as neat KBr pellets for all the derivatives. ^{1}H and ^{13}C NMR spectra were measured on a 500 MHz Bruker advanced DPX spectrometer respectively and 1,1,1,1-tetramethylsilane (TMS) is used as the internal standard for ^{1}H and ^{13}C NMR measurements. CHN analyses were carried out on an Elementar Vario MICRO cube Elemental Analyzer. All values recorded in elemental analyses are given in percentages. High Resolution Mass Spectra (HRMS) were recorded on Agilent 6538 Ultra High Definition (UHD) Accurate-Mass Q-TOF-LC/MS system using either atmospheric pressure chemical ionization (APCI) or electrospray ionization (ESI) mode.

X-ray crystallography: Single yellow crystals of **ODP1-5** were grown by slow evaporation of $CHCl_3$/hexane mixture. X-ray diffraction experiments were performed choosing high-quality crystals of approximately 0.20 × 0.15 × 0.10 mm^3 dimension. Crystallographic data collected are presented in the supporting information, Table S1. Single crystals were mounted using oil (Infineum V8512) on a glass fibre. All measurements were made on a CCD area detector with graphite monochromated MoKα radiation. The data were collected using Bruker APEXII detector and processed using APEX2 from Bruker. All structures were solved by direct methods and expanded using Fourier techniques. The non-hydrogen atoms were refined anisotropically. Hydrogen atoms were included in idealized positions, but not refined.

Determination of fluorescence quantum yield and radiative and non-radiative rate constants:[1] Solution state fluorescence quantum yields of **ODP** derivatives were calculated by relative quantum yield method as follows,

$$\Phi_s = \Phi_{ref}(\frac{I_s}{I_{ref}})(\frac{OD_{ref}}{OD_s})(\frac{n_s}{n_{ref}})^2 \qquad (1)$$

wherein, Φ_s and Φ_{ref} are the quantum yields of sample and reference respectively, I_s and I_{ref} are the area under the emission spectrum for sample and reference respectively. OD_s and OD_{ref} are the absorbances of sample and reference respectively at the excitation wavelength. $n_s$and n_{ref} are the refractive index of the solvent in which sample and reference are taken.

Radiative (k_r) and non-radiative (k_{nr}) rate constants from the singlet excited states are calculated from the fluorescence quantum yields, Φ_f.

$$\Phi_f = \frac{k_r}{k_r + k_{nr}} \qquad (2)$$

The rate constants k_r and k_{nr} can be evaluated by measuring fluorescence lifetimes (τ_f) from TCSPC measurements. The following equations depict relation between Φ_f, τ_f, k_r and k_{nr}.

$$k_r = \frac{\Phi_f}{\tau_f} \quad \text{and} \qquad (3)$$

$$k_{nr} = \frac{1 - \Phi_f}{\tau_f} \qquad (4)$$

a change in Φ_f could be attributed to the changes in either k_r/k_{nr}. Solution state relative quantum yield measurements were done using quinine sulphate in 0.05 M H_2SO_4 as the reference (Reported quantum yield Φ=0.546) exciting at 310 nm. The solid state quantum yield of crystalline ODP1-5 was measured using an integrating sphere for which the accuracy was verified using tris(8-hydroxyquinolinato)aluminium (Alq_3) as a standard and is determined to be 0.37 ± 0.04 (reported quantum yield $\Phi_f = 0.40$.[2]

Materials Science Suite: Materials Science Suite 2015-1 was utilised for the computational studies including frontier molecular orbital (FMO) analyses of monomers and dimers of ODP1-5.[3] Geometry optimization and single point energy calculations for monomers were performed at B3LYP/6-311G**+ level of theory and dimers were performed at B3LYP-D3/6-311G**+ level of theory using the crystal structure data, for FMO analysis. Energy gap is determined as the difference between energies of LUMO and HOMO. Energy level diagram is plotted using the energies obtained from FMO analyses.

Determination of degree of charge separation from Lippert-Mataga plot: The origin of solvent polarity dependent Stokes shifts could be explained using Lippert-Mataga (L-M) plots and Onsager's reaction field model, approximating that a dipole is placed at the center of a vacuum cavity in a homogeneous dielectric medium. The interaction between the solvent and fluorophores affect the energy difference between the ground and excited states and hence the dipoles associated with them. The difference in excited (μ_e) and ground state (μ_g) dipole moments could be expressed as a function of refractive index (n) and dielectric constant ($\in$) of the medium under consideration and is described as L-M equation as follows,

$$\bar{\vartheta}_A - \bar{\vartheta}_F = \frac{2}{hc}\left(\frac{\in - 1}{2\in + 1} - \frac{n^2 - 1}{2n^2 + 1}\right)\frac{(\mu_e - \mu_g)^2}{a^3} + Constant \qquad (5)$$

wherein, $\bar{\vartheta}_A - \bar{\vartheta}_F$ is the Stokes shift between absorption and emission intensity in respective solvents expressed in wavenumbers (cm^{-1}), 'h' the Planck's constant in ergs (6.626×10^{-27} ergs), 'c' the speed of light in cm/s (3×10^{10} cm/s) and 'a' the Onsager cavity radius in which the fluorophores resides.

A plot of $(\bar{\vartheta}_A - \bar{\vartheta}_F)$ against solvent polarisability parameter ($\Delta f = \left(\frac{\in - 1}{2\in + 1} - \frac{n^2 - 1}{2n^2 + 1}\right)$) yields slope equal to $\frac{2(\mu_e - \mu_g)^2}{hca^3}$, from which difference in excited and ground state dipole moment (μ_e-μ_g)

could be evaluated as, μ_e-μ_g=$\sqrt{slope \times \frac{hca^3}{2}}$. (Onsager cavity radius is estimated from theoretical calculations using B3LYP/6-311G level of theory).

L-M equation demonstrates the sensitivity of a molecule to the solvent polarity arising due to the changes in the excited state dipole moment relative to the ground state dipole moment. If the net change in dipole moment is zero (i.e. $\mu_e-\mu_g=0$), absorption and emission maxima of the chromophore should not change with solvent polarity. While, if the excited state dipole moment is larger than the ground state (i . e. $\mu_e > \mu_g$, positive slope for L-M plot), the absorption and emission maxima are anticipated to red shift with increased solvent polarity.

The degree of charge separation is estimated as follows, one Debye (1 D) unit is 1.0 x 10^{-18}esu cm. 4.8 D is the dipole moment that results from a charge separation of one unit charge (4.8 x 10^{-10}esu) by 1 Å (10^{-8} cm). Conversion of $\Delta\mu$ expressed in Debye into esu Å units is achieved by dividing by a factor of 4.8 esu^{-1}Å^{-1} which can provide the experimental charge separation in the molecule. Degree of charge separation (theoretical) in the molecule is obtained from centers of spin density distributions.

Table S1. The frontier molecular orbitals of **ODP1-5** with their calculated energies.

FMOs	ODP1	ODP2	ODP3	ODP4	ODP5	ODP5 dimer
LUMO+1	 -2.61 eV	 -2.45 eV	 -2.44 eV	 -2.56 e V	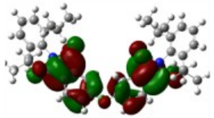 -2.44 eV	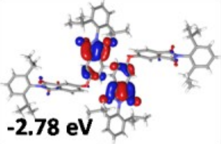 **-2.78 eV**
LUMO	 -2.79 eV	 -2.64 eV	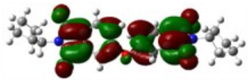 -2.63 eV	 -3.14 eV	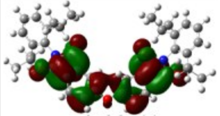 -2.66 eV	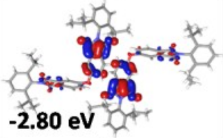 **-2.80 eV**
HOMO	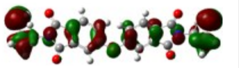 -6.96 eV	 -7.01 eV	 -6.97 eV	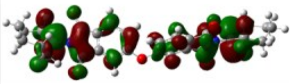 -3.48 eV	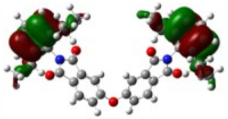 -6.70 eV	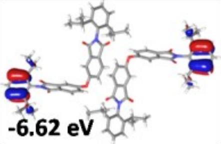 **-6.62 eV**
HOMO-1	 -6.98 eV	 -7.60 eV	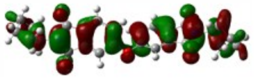 -7.48 eV	 -6.93 eV	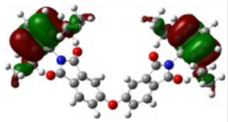 -6.71 eV	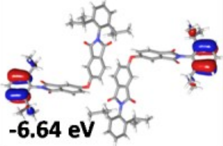 **-6.64 eV**

Table S2. Shows the percentage of intermolecular contacts of a molecule in crystalline **ODP1-5** derivatives.

Interaction	**ODP1**	**ODP2**	**ODP3**	**ODP4**	**ODP5**
H···H	31.6	19.2	24.2	25.1	21.7
C···H	18.1	17.5	17.8	16.6	13.6
O···H	8.9	1.5	7.4	6.0	4.3
C···C	0.3	1.9	0.1	2.3	2.5
C···O	38.8	59.8	48.3	47.6	55.1

Total percentage of intermolecular contacts ca. 97.7% (**ODP1**), 99.9% (**ODP2**), 97.8% (**ODP3**), 97.6% (**ODP4**), 97.2% (**ODP5**).

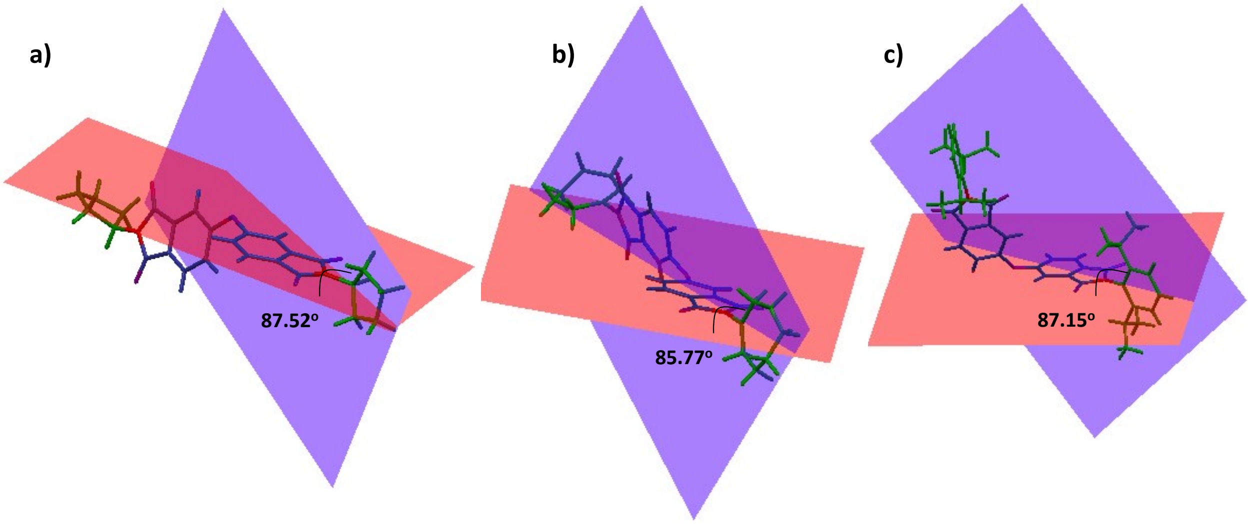

Fig. S1. Shows the dihedral angle at the imidic substitution in crystal packing of a) **ODP3,** b) **ODP4** and c) **ODP5.**

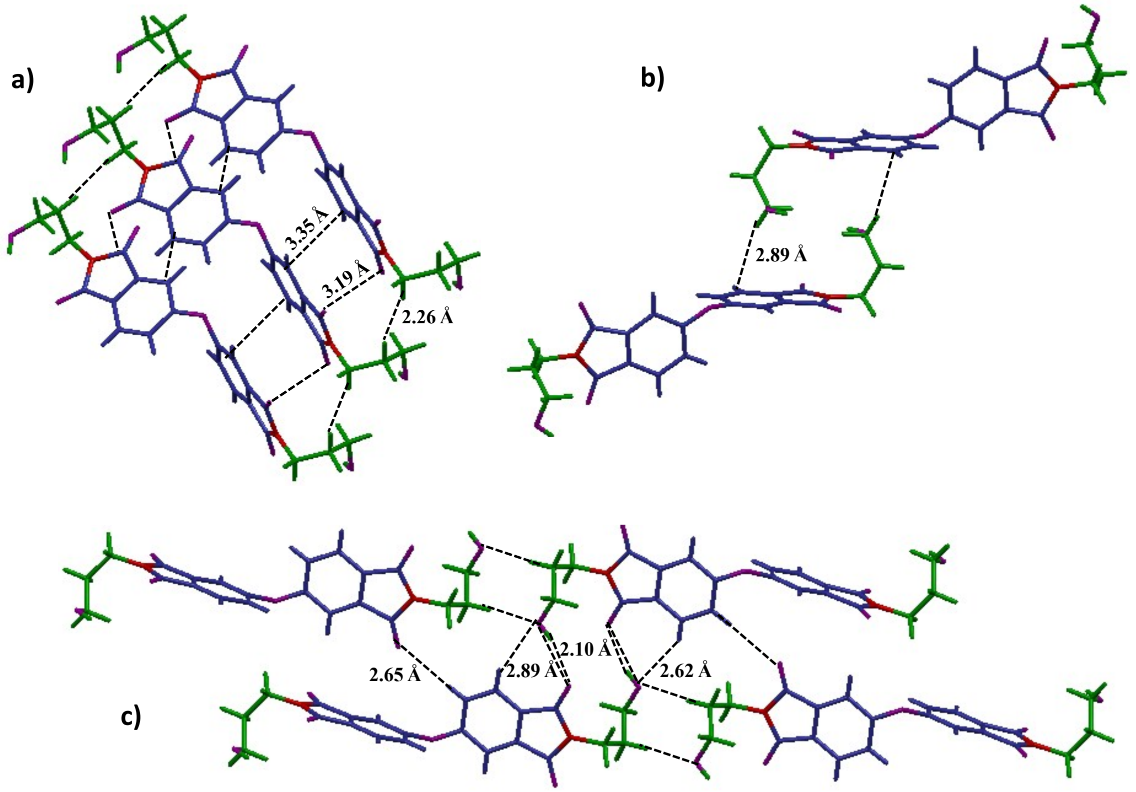

Fig. S2. Non-covalent interactions responsible for ordered packing of molecules in the crystal **ODP1**: a) H···H (2.26 Å), O···C (3.19 Å), π···π (3.35 Å); b) C-H···π (2.89 Å); c) O···H (2.10 Å), C-H···O (2.65 Å), O···O (2.89 Å), C-H···O (2.62 Å)

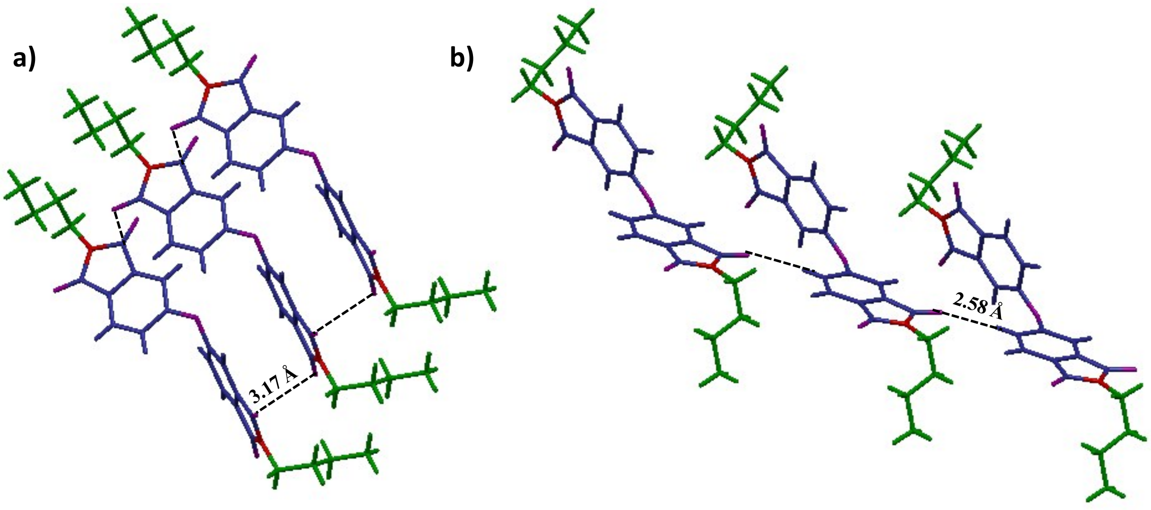

Fig. S3. Non-covalent interactions responsible for ordered packing of molecules in the crystal **ODP2**: a) C···O (3.17 Å); b) C-H···O (2.58 Å).

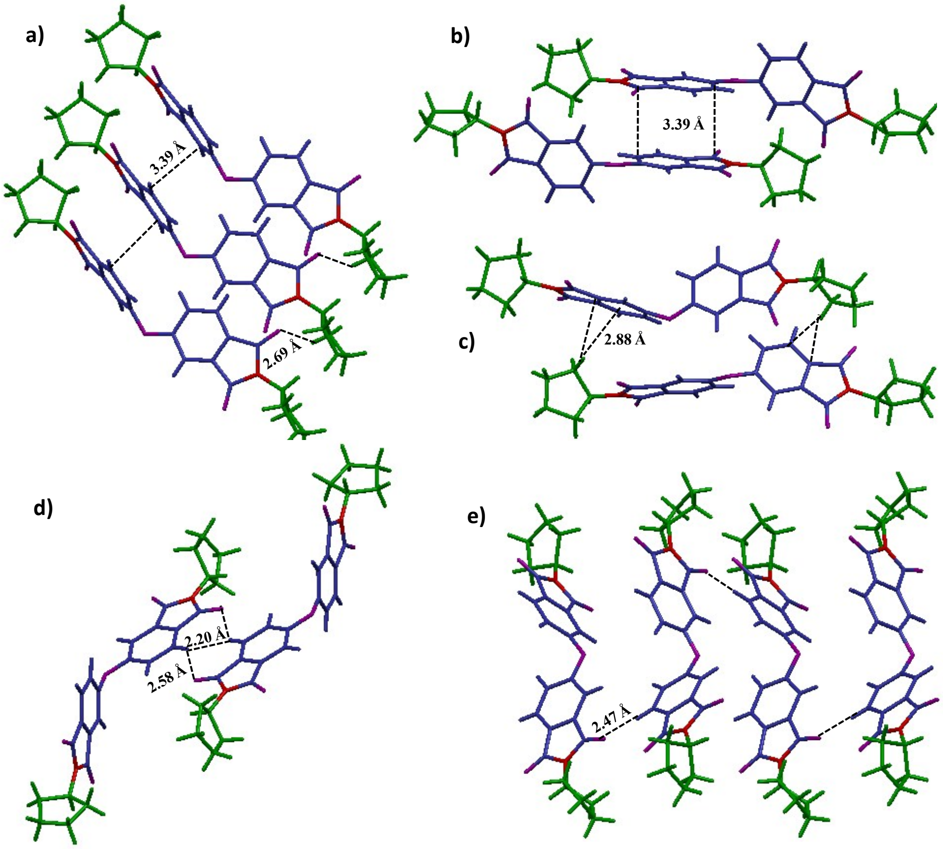

Fig. S4. Non-covalent interactions responsible for ordered packing of molecules in the crystal **ODP3**: a) π···π (3.39 Å), C-H···O (2.69 Å); b) C···C (3.39 Å); c) C···H (2.88 Å); d) C-H···O (2.58 Å), H···H (2.20 Å); e) C-H···O (2.47 Å).

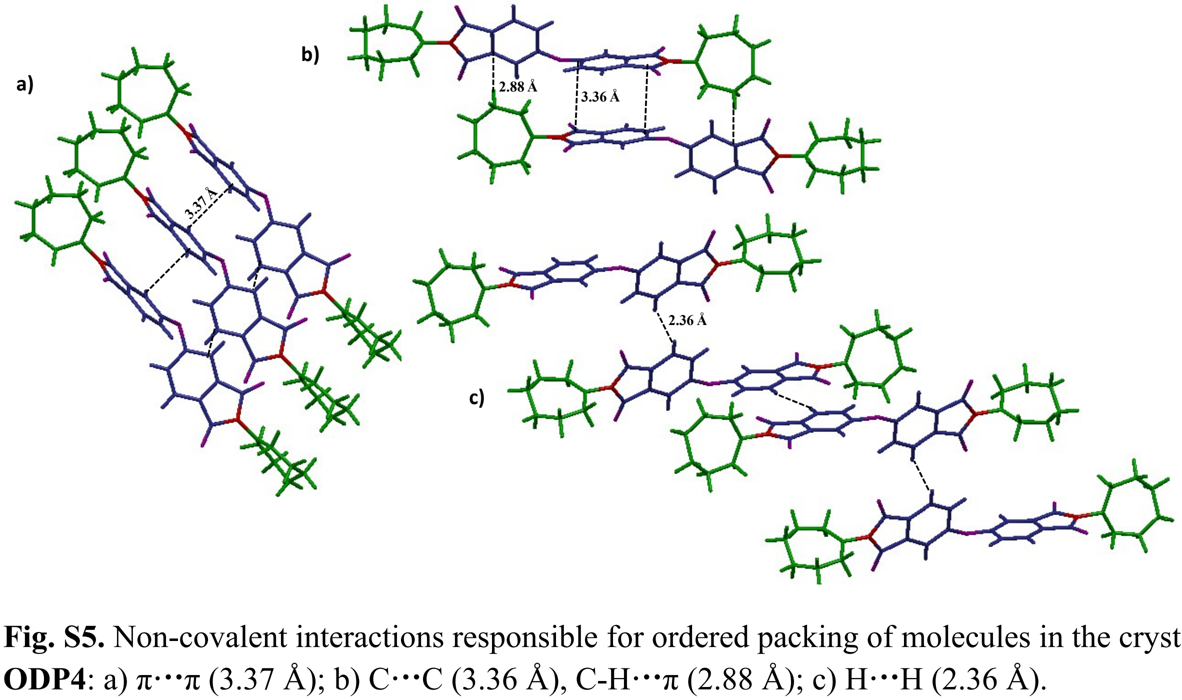

Fig. S5. Non-covalent interactions responsible for ordered packing of molecules in the crystal **ODP4**: a) π···π (3.37 Å); b) C···C (3.36 Å), C-H···π (2.88 Å); c) H···H (2.36 Å).

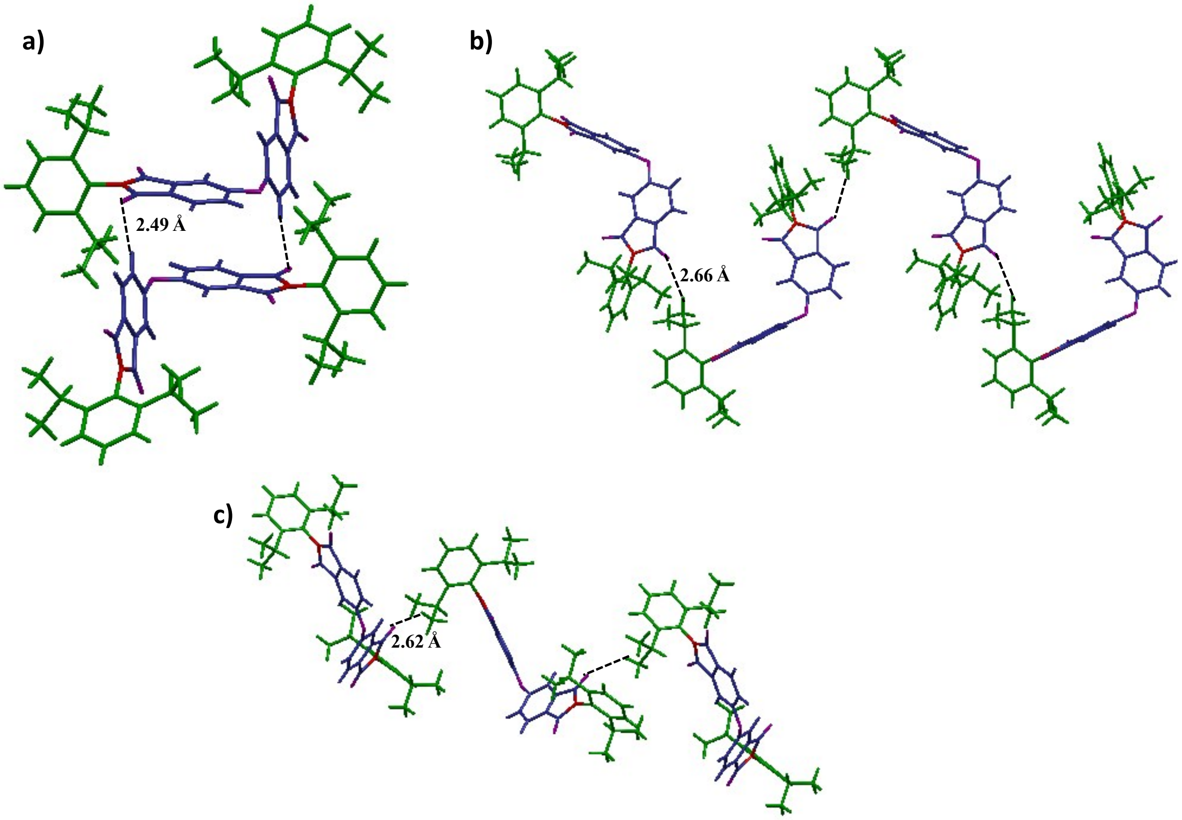

Fig. S6. Non-covalent interactions responsible for ordered packing of molecules in the crystal **ODP5**: a) C-H···O (2.49 Å); b) C-H···O (2.66 Å); c) C-H···O (2.62 Å).

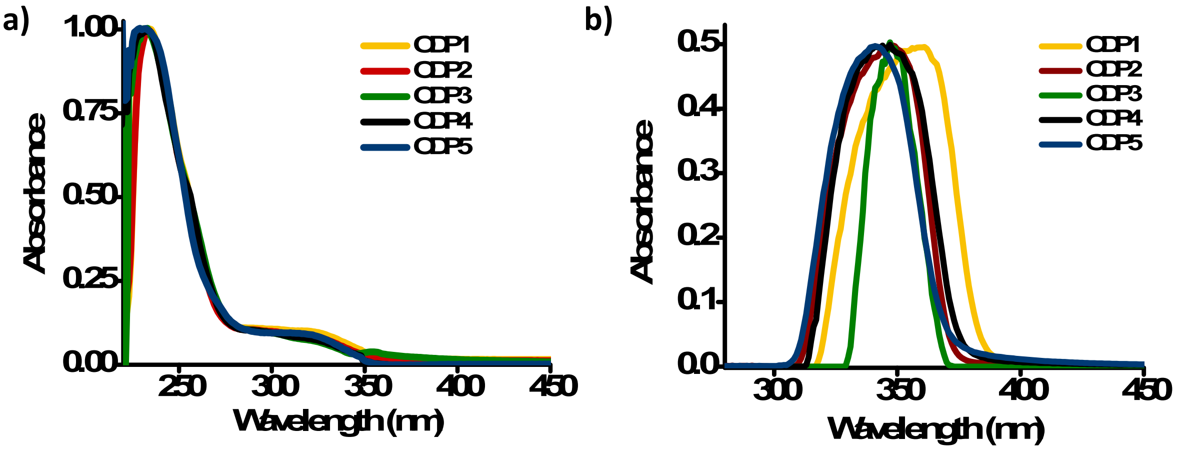

Fig. S7. Shows the normalised absorption spectra of **ODP1-5** a) solution in $CHCl_3$ (1 μM) and (b) in crystalline state**.**

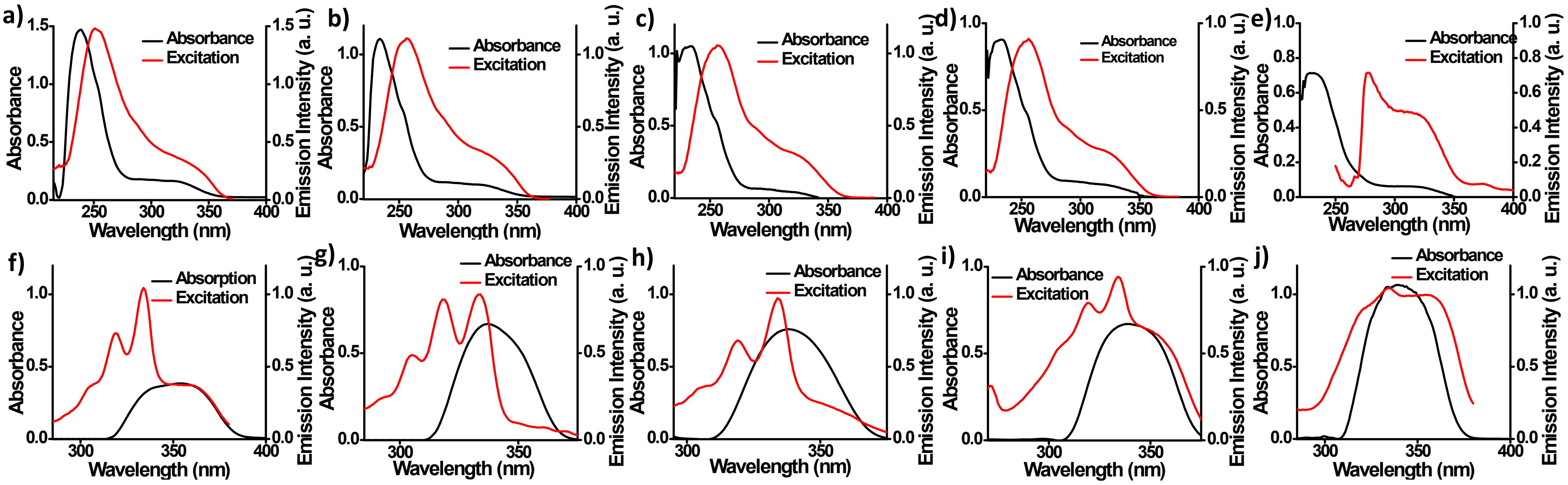

Fig. S8. Shows solution state (in $CHCl_3$) fluorescence excitation spectra of a) **ODP1**; b) **ODP2**; c) **ODP3**; d) **ODP4** and e) **ODP5;** crystalline state fluorescence excitation spectra of f) **ODP1**; g) **ODP2**; h) **ODP3**; i) **ODP4** and j) **ODP5** as compared to the corresponding absorption spectra.

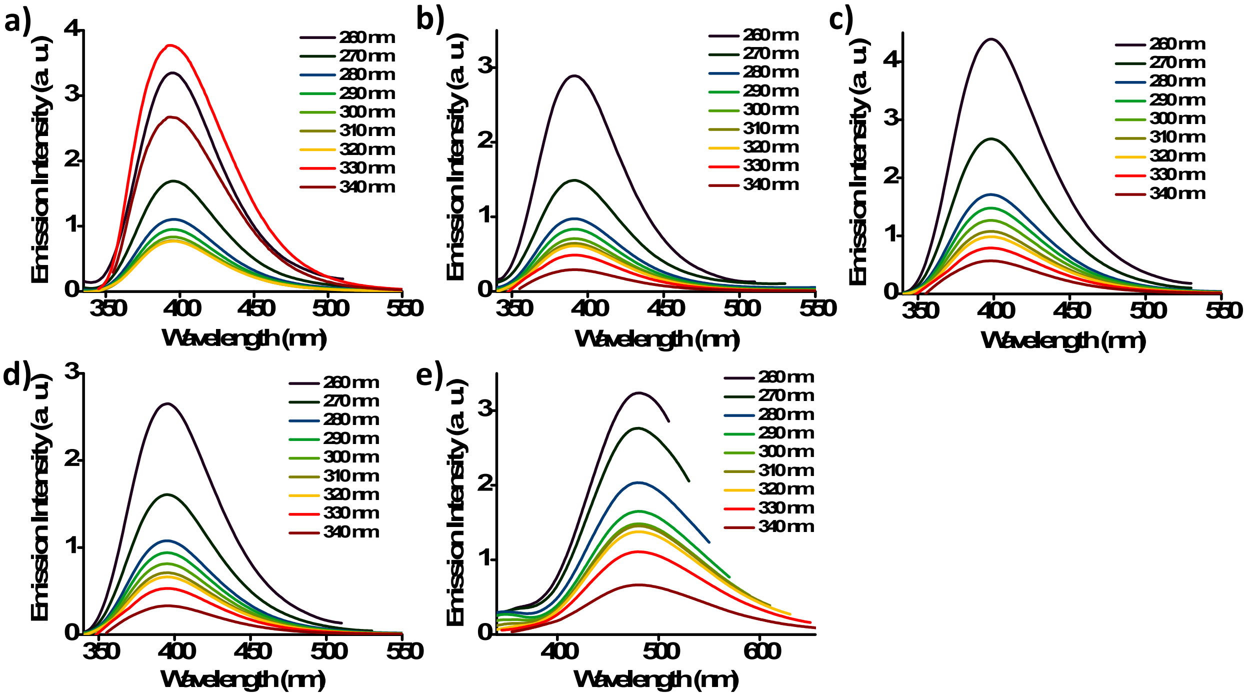

Fig. S9. Shows excitation dependent emission spectra of a) **ODP1**; b) **ODP2**; c) **ODP3**; d) **ODP4** and e) **ODP5** in solution ($CHCl_3$). Wavelengths used for excitation are indicated.

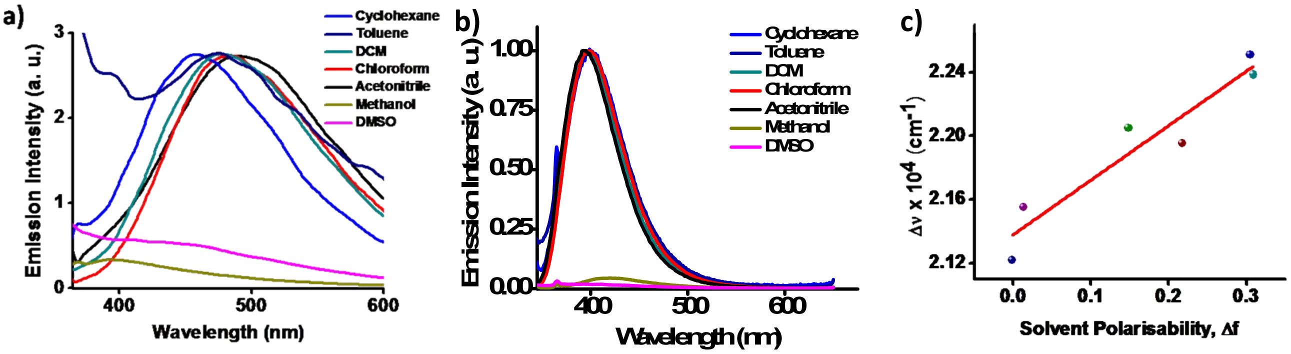

Fig. S10. Solvent dependent emission spectra of a) **ODP5** and b) **ODP2;** c) Solvent polarity dependent Lippert-Mataga plot for **ODP5**.

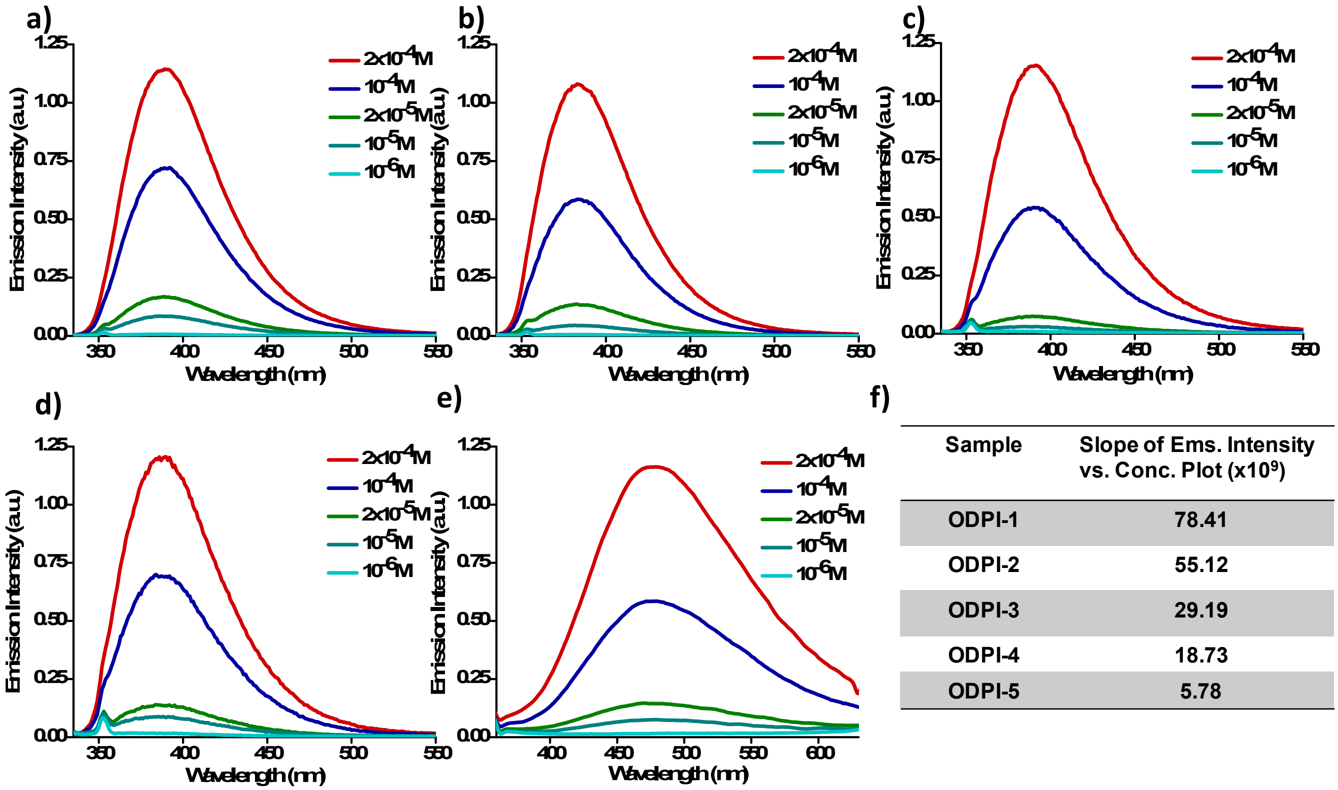

Sample	Slope of Ems. Intensity vs. Conc. Plot ($\times10^9$)
ODPI-1	78.41
ODPI-2	55.12
ODPI-3	29.19
ODPI-4	18.73
ODPI-5	5.78

Fig. S11. Concentration dependent emission spectra of a) **ODP1**; b) **ODP2**; c) **ODP3**; d) **ODP4** and e) **ODP5** in chloroform solution on excitation at 340 nm.

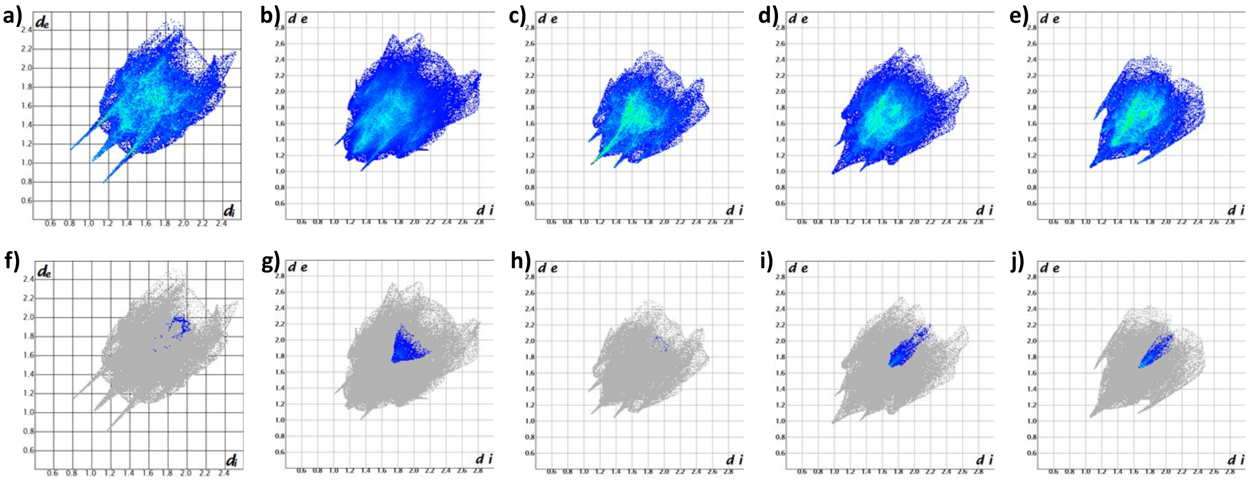

Fig. S12. Hirshfeld 2D fingerprint plots of **ODP1-5** with the region of the plots corresponding to all the interactions [a), b), c), d), e)] and C···C [f), g), h), i), j)].

Reference

1 (a) D. F. Eaton, in *Pure Appl. Chem.*, 1988, p. 1107; (b) J. R. Lakowicz, *Principles of Fluorescence Spectroscopy*, Springer US, 2007.
2 M. Cölle, J. Gmeiner, W. Milius, H. Hillebrecht and W. Brütting, *Advanced Functional Materials*, 2003, **13**, 108.
3 A. D. Bochevarov, E. Harder, T. F. Hughes, J. R. Greenwood, D. A. Braden, D. M. Philipp, D. Rinaldo, M. D. Halls, J. Zhang and R. A. Friesner, *Int. J. Quantum Chem.*, 2013, **113**, 2110.